DTU Library

Coupling colloidal quantum dots to a dielectric slot-waveguide

Israelsen, Niels M.; Lu, Ying-Wei; Andersen, Ulrik L.; Huck, Alexander

Published in:
Journal of Physics Communications

Link to article, DOI:
10.1088/2399-6528/abaacb

Publication date:
2020

Document Version
Publisher's PDF, also known as Version of record

Journal of Physics Communications

Coupling colloidal quantum dots to a dielectric slot-waveguide

IOP Publishing J. Phys. Commun. 4 (2020) 085003 https://doi.org/10.1088/2399-6528/abaacb

Journal of Physics Communications

CrossMark

OPEN ACCESS

RECEIVED
26 May 2020

REVISED
10 July 2020

ACCEPTED FOR PUBLICATION
30 July 2020

PUBLISHED
6 August 2020

PAPER

Coupling colloidal quantum dots to a dielectric slot-waveguide

Niels M Israelsen[1,2,3], Ying-Wei Lu[1], Ulrik L Andersen[1] and Alexander Huck[1]

[1] Center for Macroscopic Quantum States (bigQ), Department of Physics, Technical University of Denmark, Building 307, Fysikvej, 2800 Kgs. Lyngby, Denmark
[2] DTU Fotonik, Department of Photonics Engineering, Technical University of Denmark, Ørsteds Plads Building 343, 2800 Kongens Lyngby, Denmark
[3] Author to whom any correspondence should be addressed.

E-mail: nikr@fotonik.dtu.dk

Keywords: quantum dots, quantum emitter, gap waveguide, Purcell, dual waveguide, Density of states, LDoS

Abstract

The coupling between single photon emitters and integrated photonic circuits is an emerging topic relevant for quantum information science and other nanophotonic applications. We investigate the coupling between a hybrid system of colloidal quantum dots and propagating modes of a silicon nitride waveguide system. We furthermore explore the local density of optical states of the system by using a scanning probe technique and find that the quantum dots couple significantly to the photonic circuit. Our results indicate that a scalable slot-waveguide might serve as a promising platform in future developments of integrated quantum circuitry.

The guidance, interference and detection of light from single photon emitters on a scalable platform is of utmost importance for the development of different nanophotonic and quantum technological applications such as quantum repeaters, quantum memories and quantum computation. One of the main challenges to realize such a scalable platform is to efficiently capture the emission from single emitters onto a photonic integrated circuit in which the light guidance and interference takes place with low loss.

Most high-efficiency demonstrations have been realized in solid state systems in which the quantum emitter is directly embedded into the solid state host, e.g. defects in diamond or gallium arsenide host materials formed as cavities or waveguides [1–3]. However, the fabrication as well as the deterministic positioning of single emitters in these systems is highly nontrivial, and it is therefore interesting to consider alternative approaches based on heterogeneous (or hybrid) systems where the emitter and photonic integrated circuit constitute different material platforms [4].

One example is to use a metallic circuit where the single photon emitter is placed in the vicinity of a highly localized plasmonic field of a metallic structure, thereby largely changing the emission dynamics of the emitter and in some cases direct emission into a propagating mode of the plasmonic system [5–7]. While significant advances have been demonstrated, e.g. a Purcell enhancement of approximately 1000 [8], propagation of single plasmons in small circuits [9] and single emitter excitation of modes at the interface between metals and dielectric structures [10], the efficient coupling to a low-loss plasmonic system has yet to be realized.

To minimize the losses of the hybrid system, it might be more promising to explore the coupling of emitters to dielectric waveguides. Such a coupling and subsequent photonic propagation and linear optical manipulation has been demonstrated in multiple experiments [11–18]. In this article we explore an approach to emitter-waveguide interaction based on the coupling of colloidal quantum dots to modes supported by two closely spaced Silicon Nitride (SiN) waveguides.

The integrated platform employed in this work is schematically illustrated in figure 1(a). It comprises an optical emitter placed in the gap of two optical dielectric waveguides where the choice of material was SiN due to its low propagation losses and its CMOS compatibility. Our waveguide structure supports two transverse-magnetic (TM) photonic modes with parallel (TM_p) and anti-parallel (TM_{ap}) electric field components, as illustrated in figure 1(b). For dimension considered throughout this article, the mode index of transverse-electric (TE) modes is smaller than the mode index of the substrate and hence these modes are not considered throughout this article. Only the parallel mode TM_p is significantly located in the gap between the waveguides

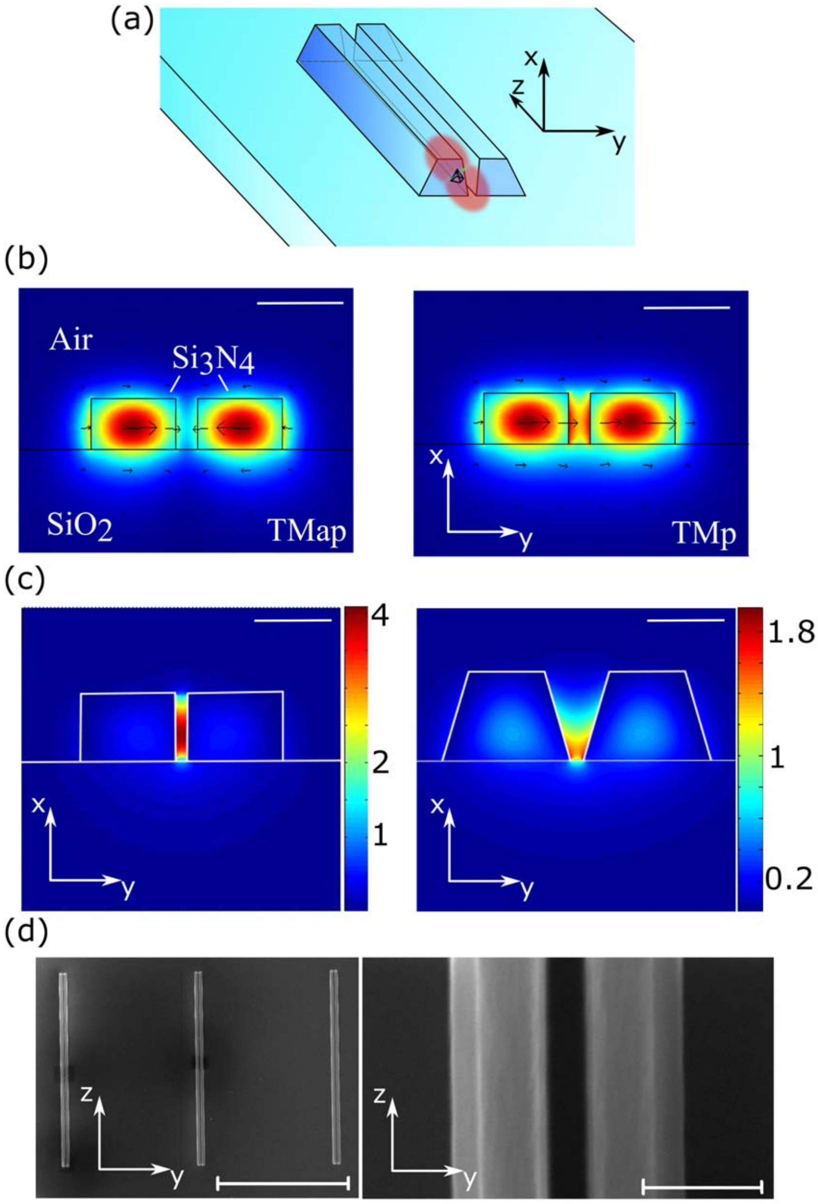

Figure 1. Coupling emitters to confined and propagating modes in a Silicon Nitride (SiN) waveguide system. (a) Schematic drawing of the heterogeneous system comprising a single emitter inside the gap of a waveguide. (b) Electric field, $|E|$, distribution of the two transverse magnetic waveguide modes of SiN. It is only the TM_p mode (right hand side) that significantly fills the gap. (c) Simulation result for the change in the decay rate of the emitter in the TM_p mode, Γ_{TM_p}/Γ_0, for perfectly parallel waveguides (left) and slanted waveguides (right). (d) Scanning electron microscopy image of the waveguide in full size (left) and a zoom (right) where the slanted walls become visible. The scale bars are: (b) 400 nm, (c) 200 nm, (d) 10 μm left hand side and 300 nm right hand side.

and due to this localization, we expect a strong interaction between the waveguide structure and an embedded emitter to occur in the gap. The interaction strength can be quantified by the decay rate enhancement Γ_{TM_p}/Γ_0 [19] and the mode coupling efficiency $\beta = \Gamma_{TM_p}/(\Gamma_0 + \Gamma_{TM_p})$, where Γ_{TM_p} and Γ_0 are the decay rates of the emitter when placed at the mode field maximum in the gap and in vacuum, respectively. It is assumed that the emitter transition dipole moment is parallel to the electric field vector. For waveguide dimensions of 250 nm $\times$ 175 nm (width x height) and a gap size of 30 nm, we obtain a theoretical enhancement of the decay rate by almost a factor of four which means that around 80% of the emitters fluorescence will be captured by the propagating TM_p mode (see left plot of figure 1(c) [20]. The actual fabricated waveguide geometry is however slanted, as shown in the right plot of figure 1(c). In such a system, the mode localization in the gap decreases and hence the expected maximum achievable coupling rate is lower. For the dimensions shown in the figure, we can at most expect an enhancement in the decay rate of a factor about two and $\beta \approx 60\%$.

The waveguides were fabricated by depositing a layer of SiN on a fused silica substrate using low power chemical vapor deposition, followed by electron beam lithography and dry etching. Scanning electron microscope images of the fabricated slanted waveguide structures are shown in figure 1(d). The cross sectional

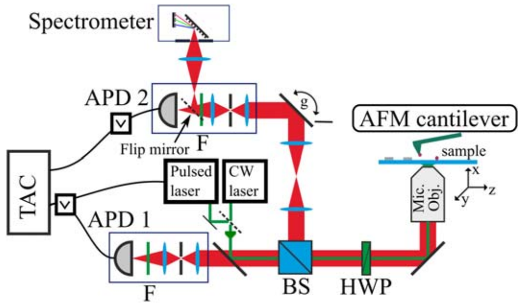

Figure 2. Schematic of the experimental setup. See text for description. AFM: Atomic force microscope. TAC: time to amplitude converter. APD1 and APD2: avalanche photo diode detection channel 1 and 2, respectively. g:galvanometric mirror. BS:50-50 beam splitter. HWP:half waveplate. F: Notch-Filter with low transmission at 532 $\pm$ 15 nm.

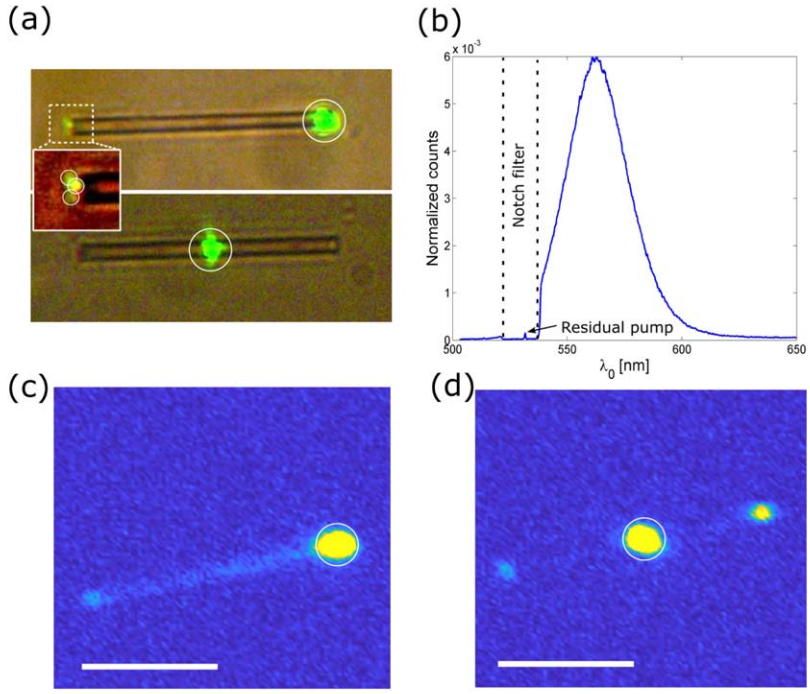

Figure 3. Characterization of the system. (a) A wide field microscope image of the waveguide system when green laser light (white circle) is focused onto the waveguide end (upper image) or the middle (lower image). (b) Photoluminescence spectrum of the CdSe colloidal quantum dots. (c) and (d) Confocal map of the system under green light excitation where the excitation is performed onto the end (c) or the middle (d) of the waveguide. The location of the laser is marked with a white circle and the scale bars are 8 μm.

dimensions are similar to the one simulated in figure 1(c) and the length is 15 μm. We interrogate the system using the confocal microscope schematically shown in figure 2. For the excitation of the quantum dots we used a continuous wave (cw) or a pulsed laser operating at the wavelength of 532 nm and linear polarized. The fluorescence emission from the sample is collected by two optical channels and detected with avalanche photo diodes (APDs). The channel APD1 is aligned with the excitation laser while the channel of APD2 can be scanned using galvanometric mirrors, thereby allowing for fluorescence imaging with a fixed excitation spot. We used an oil immersion objective with a numerical aperture of 1.4 to focus and collect the light. For experiments on measuring the quantum dot emission, we inserted a 532 nm notch filter with a 15 nm bandwidth to block the excitation laser.

We first investigate the propagation of guided modes excited by cw green laser light. As illustrated in figure 3(a), we launch the green laser beam into the waveguide structure by focusing the light onto the end facet of the waveguide system. Due to the structural asymmetry at the end facet, photons are coupled from the laser beam into the waveguide system and propagate along to its distal end at which it scatters the photons out. A zoom of the emitted light indicates three emission spots associated with propagating modes supported by the waveguide system. The intensity measurements shown here are not suitable to quantify in more detail the exact mode excited by the laser, propagating along the waveguide structure and coupling back to free space. However, we note that the the linear polarized laser used in the experiment is more likely to couple into the TM_p mode with a symmetric electric field profile in the transverse plane, but scattering at the input facet or upon nanoscopic structural imperfections along the waveguide might also excite the TM_{ap} mode. Nevertheless, this experiment verifies the existence of propagating modes of our waveguide structure. As also illustrated in figure 3(a), when shining light onto the middle of the waveguide system, no propagating mode was excited and thus the ends of the waveguide remained dark.

As a next step we wish to locate emitters inside the gap and explore the maximum possible coupling to the propagating TM_p mode. We use core CdSe colloidal quantum dots of size 2.6 nm–3.0 nm dissolved in toluene and at room temperature emitting light in a broad spectrum with a center wavelength around 565 nm (see emission spectrum in figure 3(b)). The dot solution was ultra-sonicated for 2 minutes before being spin coated onto an ultra clean waveguide sample. We used 20 μl of the quantum dot solution while spinning with a speed of 1000rpm which was increased to 8000rpm after 10 s. The final sample contained an ensemble of quantum dots with random orientation and uniformly distributed along the waveguide structure, as confirmed by a confocal scan of the system. Coupling is only expected for quantum dot emitters with a component of their transition dipole moment parallel to the electric field of the waveguide modes.

The confocal scans presented in figures 3(c), (d) illustrate our results on coupling emitters to the propagating modes. We locate the cw green excitation laser either at the end (figure 3(c)) or in the middle (figure 3(d)) of the waveguide structure while scanning an area of 20 μm $\times$ 20 μm from which the fluorescence light is measured (the green light was filtered out in this experiment using a notch filter). The brightest fluorescence spot is seen from direct quantum dot emission where the laser is located. From excitation of emitters in the middle of the waveguide, it is clear that some of the fluorescence light is captured by the waveguide modes, propagates along the structure and is re-emitted at the ends. When we excite at the end of the waveguide a part of the green light is also launched into propagating waveguide modes. Then, emitters are also excited along the waveguide as the waveguide appears as a bright straight line in the fluorescence image. This effect is not significant when locating the laser at the center of the waveguide as in this case the excitation beam is not coupled into the waveguide (see figure 3(a)). It means that at the waveguide end facet it is possible to convert the excitation beam into a propagating waveguide mode before it excites the emitters at a location that is remote to the focused spot of the excitation beam.

To investigate whether the dynamics of the emitters is changed due to the coupling to the waveguide mode, we conducted some lifetime measurements of the emitters. However, since the density of emitters along the waveguide was large, we could not conclude from the acquired measurements whether a change in lifetime is due to coupling to the propagating modes or simply due to the high density of colloidal quantum dots [21–23]. To avoid these density-dependent effects we performed measurements with a few emitters using a scanning-probe fluorescence lifetime imaging microscope [24, 25], by which an image of the emitter's lifetimes across the waveguide system could be constructed with nanometer scaled spatial resolution. We include the functionality in our setup by coaxially aligning the silicon cantilever tip of an atomic force microscope (AFM, NT-MDT SMENA) to the focused excitation laser in our confocal microscope, as schematically illustrated in figure 2. In our realization, we scanned the waveguide sample in the transverse plane while operating the AFM in tapping mode and collected fluorescence photons through the objective towards the apparatus measuring the fluorescence counts and the lifetime. With this technique we were able to make a nanoscaled map of the lifetimes associated with a few emitter attached to the AFM tip in varying environments in which the local density of optical states changes.

Emitters were deposited onto the cantilever tip by dragging it in contact mode through a region with a high concentration of CdSe quantum dots on a reference sample. After removing the AFM cantilever from the region of quantum dots, we observed emitter fluorescence when exciting the tip alone, thus confirming that a few quantum dots have been picked up. Using this tip and changing back to the waveguide sample cleaned with tuluene and de-ionized water, we produced a real image and a fluorescence image of the waveguides as shown in figure 4(a). We note that the count rate is much lower atop the waveguides than at the substrate base. This observation we attribute to the fact that in the close vicinity the waveguides modify the quantum dot emission and lower the coupling to the objective.

We next investigate the potential coupling of the quantum dots to the waveguides by exploring the lifetimes of the quantum dots across the waveguide structure. Towards this end, we carry out a 1 μm $\times$ 4 μm scan of the quantum dots across the waveguide system and simultaneously record a topographic, a fluorescence and a lifetime image. The results are illustrated in figures 4(c)–(f). Note that these measurements are performed with the AFM operating in tapping mode which means that the cantilever oscillates with an amplitude of approximately 70 nm (with a frequency of 178 kHz) in a direction orthogonal to the scanning plane. The obtained results are therefore averaged over these oscillations. We also note from the measured results in figures 4(c)–(d) that the fluorescence image was displaced from the topographic image by approximately 1 μm. This is caused by the fact that the quantum dots were not attached exactly at the apex of the cantilever tip but at

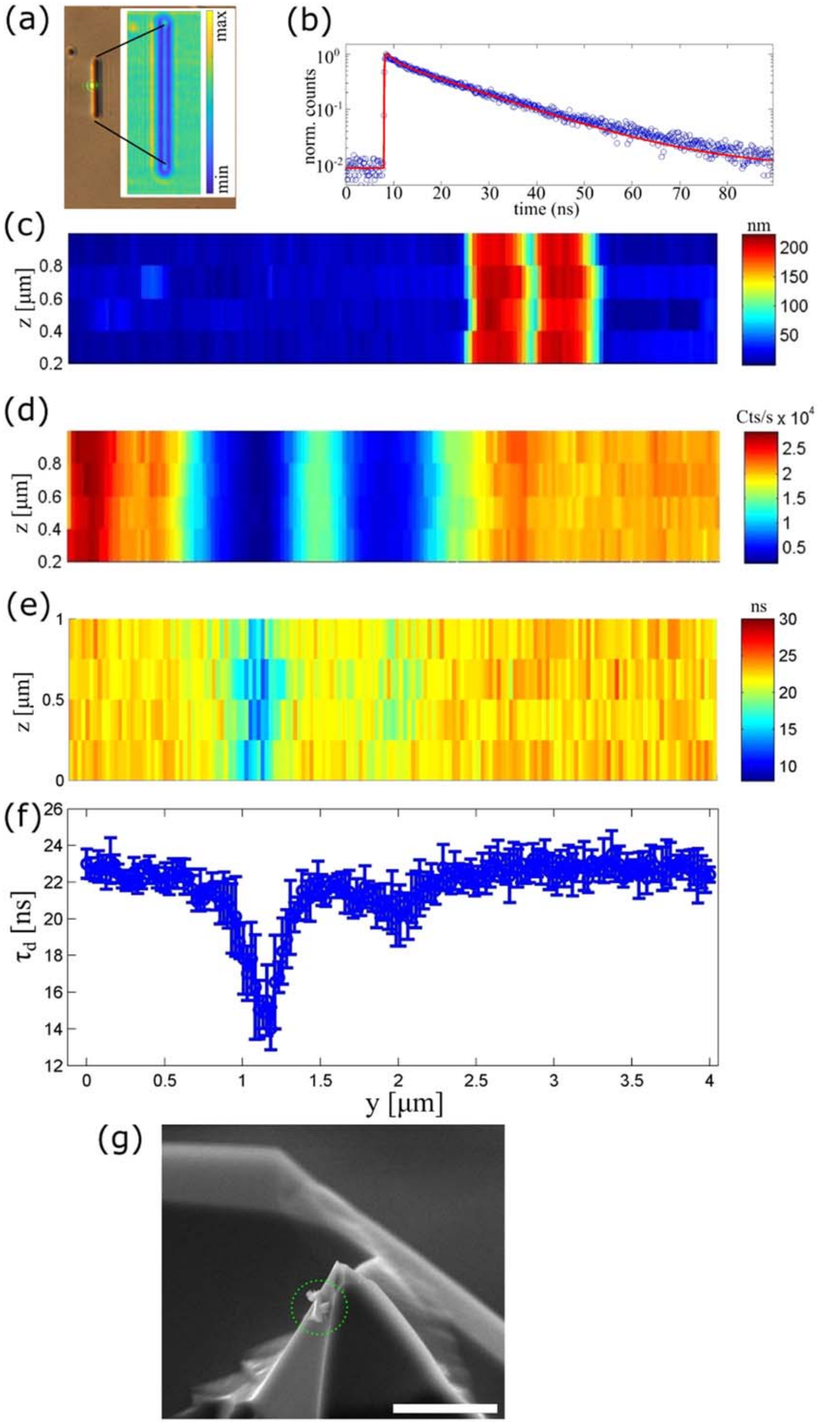

Figure 4. Characterization of the hybrid quantum dot-waveguide system using the scanning probe technique. (a) An optical image of the entire waveguide structure. Inset: A fluorescence image of the same system. (b) Fluorescence decay curve, where blue circles are experimental data while the red curve is a fit with a multi-exponential function with lifetime τ_d. (c) AFM height measurement of the waveguide. (d) A fluorescence image of the quantum dot while it is scanned across the waveguide. (e) Lifetime measurements of the quantum dots as they are scanned across the waveguide. (f) Lifetime measurement averaged along the z-direction in (e). (g) A scanning electron microscope image of the cantilever tip with quantum dots on the side of the tip indicated by the green circle. The scale bar is 5 μm.

the side of the tip (which was confirmed by a further investigation with scanning electron microscope, see figure 4(g)).

To estimate the lifetimes, we simulate the quantum dot decay mechanism by employing a three level model which accounts for phonon decays followed by photonic decay. The decay pattern could be modelled as [26]

$$I_{tot}(t) = I_1(t) + I_2(t) + I_{offset}, \tag{1}$$

where

$$I_i(t) = A_i \frac{k_{ph,i} k_i}{-k_i + k_{ph,i}} (-e^{-(t-\tau_0)/\tau_{ph,i}} + e^{-(t-\tau_0)/\tau_i}). \tag{2}$$

Here, A_i is the amplitude, $\tau_i = 1/k_i$ and $\tau_{ph,i} = 1/k_{ph,i}$ are the lifetimes associated with the photonic and phononic decays, respectively. The lifetime for the system was then defined as $I_{tot}(\tau_d) = e^{-1} I_{tot}(t = \tau_0)$. The offset, I_{offset}, is found by averaging the counts before the arrival of the excitation pulse at τ_0. Figure 4(b) shows an example of a lifetime measurement where we have fitted the multi-exponential function in equation (1) to the experimental data [27, 28].

In figures 4(e) and (f) we plot the measured lifetimes, τ_d, across the waveguide structure. It is clear that the lifetime and thus the quantum dot dynamics is modified due to the presence of the waveguides. The lifetime is decreased by up to a factor of approximately 1.5, thus indicating a significant coupling to the waveguide. However, it is also clear that the strongest coupling does not occur in the gap between the waveguides as expected (see figure 1(c)). The missing coupling in the gap is attributed to the fact that the cantilever blunted by the multiple scans performed throughout the experiment (see figure 4(g)), the conical cantilever shape, and that the quantum dots are positioned at the side of the tip. Hence the quantum dots may not go into the gap during the scan. A local modification of the waveguide modes due to the presence of the cantilever tip might also impact the observable emitter dynamics, which is not considered in our model. On the other hand, the quantum dots will get very close to the outer wall of one of the waveguides as the cantilever is scanned across. This explains the asymmetry of the lifetime scan in figures 4(e) and (f). Therefore, although we have not experimentally proven a strong coupling between the emitter and the propagating modes, the emitter is clearly coupling significantly to the waveguiding system. This indicates that a single quantum dot eventually embedded into the gap will be efficiently coupled to the propagating modes.

To observe a change in the lifetime of the quantum dots coupled to the propagating modes, it is critical to be able to attach the quantum dots exactly at the apex of the cantilever tip. This turned out to be a huge challenge with the current system since we have no means of observing in real time the attaching process. An effective solution that will facilitate the process and measurement is to combine the AFM and the confocal microscope with a scanning electron microscope. This would allow real-time imaging of the attaching process and at the same time monitoring the fluorescence from the quantum dots.

In conclusion, we have explored the interaction of quantum dots with modes of a photonic waveguide system. In particular, we have demonstrated the excitation of propagating waveguide modes by quantum dots, and we have witnessed an efficient coupling between the two systems. As an outlook, we suggest to improve the controllability in assembling the system, to reduce the size of the gap for increasing the coupling rate and to test the system with stable emitters such as single quantum dots or color centers in diamond. Once developed, the platform can potentially serve as a building block for scalable nanoscale photonics [29], quantum dot based bio-analysis [30] and scalable quantum information processing [31].

Acknowledgments

We greatly acknowledge funding from the Danish Research Council through a Sapere Aude grant (DIMS, Grant No. 4181-00505B).

ORCID iDs

Niels M Israelsen https://orcid.org/0000-0001-9632-7902

References

[1] Kim H, Bose R, Shen T C, Solomon G S and Waks E 2013 *Nat. Photonics* **7** 373
[2] Hausmann B J *et al* 2012 *Nano Lett.* **12** 1578
[3] Evans R E *et al* 2018 *Science* **362** 662
[4] Benson O 2011 *Nature* **480** 193
[5] Akimov A V, Mukherjee A, Yu C L, Chang D E, Zibrov A S, Hemmer P R, Park H and Lukin M D 2007 *Nature* **450** 402
[6] Huck A, Kumar S, Shakoor A and Andersen U L 2011 *Phys. Rev. Lett.* **106** 096801
[7] Kumar S, Huck A and Andersen U L 2013 *Nano Lett.* **13** 1221
[8] Akselrod G M, Argyropoulos C, Hoang T B, ciraci C, Fang C, Huang J, Smith D R and Mikkelsen M H 2014 *Nat. Phot.* **8** 835
[9] Kumar S, Kristiansen N I, Huck A and Andersen U L 2014 *Nano Lett.* **14** 663
[10] Kumar S and Bozhevolnyi S 2019 *A C S Photonics* **6** 1587
[11] Türschmann P, Rotenberg N, Renger J, Harder I, Lohse O, Utikal T, Götzinger S and Sandoghdar V 2017 *Nano Lett.* **17** 4941
[12] Khasminskaya S *et al* 2016 *Nat. Photonics* **10** 727

[13] Davanco M, Liu J, Sapienza L, Zhang C Z, De Miranda Cardoso J V, Verma V, Mirin R, Nam S W, Liu L and Srinivasan K 2017 *Nat. Commun.* **8** 1
[14] Elshaari A W, Zadeh I E, Fognini A, Reimer M E, Dalacu D, Poole P J, Zwiller V and Jöns K D 2017 *Nat. Commun.* **8** 1
[15] Kim J H, Aghaeimeibodi S, Richardson C J, Leavitt R P, Englund D and Waks E 2017 *Nano Lett.* **17** 7394
[16] Osada A, Ota Y, Katsumi R, Kakuda M, Iwamoto S and Arakawa Y 2019 *Physical Review Applied* **11** 1
[17] Katsumi R, Ota Y, Osada A, Yamaguchi T, Tajiri T, Kakuda M, Iwamoto S, Akiyama H and Arakawa Y 2019 *APL Photonics* **4** 036105
[18] Kim S, Duong N M H, Nguyen M, Lu T J, Kianinia M, Mendelson N, Solntsev A, Bradac C, Englund D R and Aharonovich I 2019 *Advanced Optical Materials* **7** 1
[19] Chen Y, Nielsen T R, Gregersen N, Lodahl P and Mørk J 2010 *Phys. Rev.* B **81** 125431
[20] Robinson J T, Manolatou C, Chen L and Lipson M 2005 *Phys. Rev. Lett.* **95** 143901
[21] Kagan C R, Murray C B and Bawendi M G 1996 *Phys Rev.* B **54** 8633
[22] Kawata G, Ogawa Y and Minami F 2011 *Jour. of Appl. Phys.* **110** 064323
[23] Hartmann L *et al* 2012 *ACS Nano* **6** 9033
[24] Michaelis J M J, Hettich C and Sandoghdar V 2000 *Nature* **405** 325
[25] Schell A W, Engel P, Werra J F M, Wolff C, Busch K and Benson O 2014 *Nano Lett.* **14** 2623
[26] Santori D F C and Yamamoto Y 2010 *Single Photon Devices and Applications* (Boschstrasse 12, 69469 Weinheim, Germany: Wiley-VCH) 978-3-527-40807-8
[27] Salman A A, Tortschanoff A, van der Zwan G, van Mourik F and Chergui M 2009 *Chem. Phys.* **357** 96
[28] Knowles K E, McArthur E A and Weiss E A 2011 *ACS Nano* **5** 2026
[29] Harris N C, Bunandar D, Pant M, Steinbrecher G R, Mower J, Prabhu M, Baehr-Jones T, Hochberg M and Englund D 2016 *Nanophotonics* **5** 456
[30] Altintas Z, Davis F and Scheller F W 2018 *Biosensors and Nanotechnology Applications in Health Care Diagnostics* (111 River Street, Hoboken NJ 07030, USA: John Wiley & Sons, Ltd) 9 183–199
[31] Slussarenko S and Pryde G J 2019 *Applied Physics Reviews* **6** 041303